Enzymatic and structural characterization of non-peptide ligand–cyclophilin complexes

George Kontopidis, Paul Taylor and Malcolm D. Walkinshaw*

Structural Biochemistry Group, Department of Biochemistry, The University of Edinburgh, Michael Swann Building, King's Buildings, Edinburgh EH9 3JR, Scotland

Correspondence e-mail: m.walkinshaw@ed.ac.uk

Piperidine ligands are described that provide the first examples of non-peptidic ligand structures for the cyclophilin family of proteins. Crystal structures of two ligand complexes are compared with the unliganded protein and show ligand-induced changes in side-chain conformation and water binding. A peptidylprolyl *cis–trans*-isomerase assay showed the dissociation constants of the two ligands to be 320 and 25 mM. This study also provides the first published data for both enzymatic activity and three-dimensional structure for any protein–ligand complex that binds with a high-millimolar dissociation constant. The structures may be of relevance in the field of drug design, as they suggest starting points for the design of larger tighter-binding analogues.

1. Introduction

Cyclophilins belong to the family of peptidyprolyl-isomerase (PPIase) enzymes that regulate protein folding and transport (Galat & Metcalfe, 1995; Lilie *et al.*, 1993). Cytosolic human cyclophilin A (hCypA) is the most abundant form and is the target for the immunosuppressant drug cyclosporin A, which is used to prevent organ rejection after transplant operations (Beveridge & Calne, 1995). Inhibition of various cyclophilin isoforms may also be of potential therapeutic value in a diverse range of disease areas. The discovery that inhibition of cyclophilin prevents its incorporation into the HIV protein coat suggests that families of inhibitors unrelated to the immunosuppressant cyclosporins may have anti-HIV activity. Parasitic nematodes require a variety of cyclophilins to process collagen coat proteins at different stages in their life cycle (Page *et al.*, 1995) and the development of species-specific cyclophilin inhibitors may also provide a route to anti-parasitic drugs. The molecular structure of cyclophilin provides a good template for the design of novel ligands, as the active site seems to conserve its conformation when bound to a variety of large and small peptide ligands (Taylor *et al.*, 1997).

There has been growing interest in the use of NMR (Meyer & Peters, 2003; Glen & Allen, 2003) and protein X-ray crystallography (Blundell *et al.*, 2003) as tools for the discovery of new ligands. These two structural approaches are particularly good at identifying weakly binding ligands and complement the high-throughput screening techniques which usually restrict the search for novel ligands to those that bind with low-micromolar dissociation constants (Bleicher *et al.*, 2003). Surveys of oral drug molecules (Davis & Teague, 1999) and protein–ligand complex structures (Bohm & Klebe, 1996) suggest that ligands that bind with better than micromolar dissociation constants will typically consist of more than 20 non-H atoms and form some three hydrogen bonds. It is

DOI: 10.1107/S0907444904000174 **479**

therefore of considerable interest to obtain more detailed structural and binding information on the nature of weaker protein–ligand interactions which may also provide a useful starting point for drug-lead development.

There is a paucity of data in the literature on the inhibitory and binding properties of weakly binding ligands, although X-ray crystallographic studies of protein–solvent complexes provide some structural insights (Ringe & Mattos, 1999). Cross-linked protein crystals have been soaked in pure solvents, including benzene, dimethylformamide and acetonitrile. The refined X-ray structures provide a map of potential ligand-binding sites (Allen *et al.*, 1996). There are numerous examples of other solvent molecules being sequestered in the protein crystal lattice and the current Protein Data Bank (Berman *et al.*, 2000) has over 30 examples of proteins forming complexes with dimethylsulfoxide, 20 examples of methanol complexes and over 160 examples of glycerol complexes formed during flash-freezing experiments in which crystals are soaked in solutions containing high concentrations of glycerol. It is clear from these examples that when the concentration of small-molecule solvent ligands is high (typically in the range 1.5–15 M), the law of mass action can act to form a complex even if the dissociation constant is very large. In none of these crystalline protein–ligand complexes is the dissociation constant known. The work described in this paper provides first examples of non-peptide ligands for cyclophilin and the accompanying enzymatic data fills an important gap in our understanding of how weak (millimolar) ligands bind.

2. Materials and methods

2.1. Enzymatic assay

PPIase activity is assessed using the α-chymotrypsin-coupled enzymatic assay (Kofron *et al.*, 1991). α-Chymotrypsin selectively hydrolyses the C-terminal p-nitroanilide bond of the substrate in the *trans X*-Pro conformer only. This hydrolysis releases the chromophore 4-nitroaniline, the accumulation of which is recorded by measuring the absorbance at 400 nm as a function of time. The *trans*-peptide is cleaved within the deadtime, so this cleavage does not contribute to the total reaction time. The substrate (a stock solution of 100 mM) was dissolved in LiCl/trifluoroethanol (TFE). The experiment took place at 277 K. Constant temperature was maintained within the cuvette using a Peltier (PTP-1) temperature-control unit. A mini magnetic stirring system (Telemoduel, Variomag) was used to mix the solution in the cuvette after the addition of the substrate. A Perkin–Elmer UV/Vis Lambda 20 spectophotometer was used. The substrate was N-succinyl-Ala-Ala-Pro-Phe-p-nitroanilide (Bachem AG). hCypA solution was freshly prepared before the experiment from frozen stock solution at the appropriate concentration by dilution in 50 mM HEPES, 100 mM NaCl pH 8.0 (buffer A). In a typical experiment, 90 µl of 2.5–30 nM hCypA was made up to 2520 µl with buffer A in a 3 ml glass cuvette. The cuvette was then preincubated for 30 min on ice. Immediately before the assay, 300 µl of chymotrypsin (Sigma)

solution (50 mg ml^{-1} in 10 mM HCl) was added, followed by 90 µl of a 3.7 mM stock solution of Suc-Ala-Ala-Pro-PNA in LiCl (470 mM)/TFE. The reaction progress was monitored by the absorbance change at 400 nm that accompanies the hydrolysis of the amide bond and the release of 4-nitroaniline product.

2.2. Crystallization and structure determination

Recombinant hCypA was concentrated to 14 mg ml^{-1} in 20 mM HEPES, 100 mM NaCl, 0.02%(w/v) NaN$_3$. Crystals of hCypA were grown by vapour diffusion at 290 K by the hanging-drop method. The precipitating solution in the well consisted of 100 mM Tris–HCl pH 8.0, 22%(w/v) PEG 8000, 5%(v/v) DMSO, 0.02% NaN$_3$. The initial 8 µl drop consisted of 50 mM Tris–HCl pH 8.0, 11%(w/v) PEG 8000, 2.5%(v/v) DMSO, 0.02% NaN$_3$, 0.4 mM hCypA.

The ligand was introduced into the crystal (0.2 × 0.1 × 0.025 mm) using a stepwise-soaking procedure in which the DMSO concentration was gradually reduced and the ligand concentration was gradually increased. This procedure was required to prevent crystal damage and also to prevent competition by DMSO binding at the active site. In the first step, a single crystal of hCypA was soaked in a precipitating solution containing 20 mM ethyl-1-piperidine glyoxylate (ETPIPG) and a reduced (4%) concentration of DMSO. After 1 h, the crystal was transferred to a fresh soaking solution containing 40 mM ligand and 3% DMSO. The crystal was transferred a total of six times over a period of 6 h. The final soak was for 2.5 h in a solution containing no DMSO and 180 mM ETPIPG. The same stepwise-soaking procedure was followed for a crystal (0.3 × 0.15 × 0.05 mm) soaked in 1-acetyl-3-methylpiperidine (ACMPIP). The initial ligand concentration of 50 mM was again increased over six steps to a final concentration of 300 mM.

Flash-freezing of the crystal in liquid nitrogen was carried out after soaking in a cryoprotectant solution consisting of 100 mM Tris–HCl pH 8.0, 22%(w/v) PEG 8000, 0.02% NaN$_3$, 180 mM ligand and 26% glycerol. Data were collected using a Nonius rotating-anode generator. The resolution of the data was improved when data from the same crystal were collected at Daresbury SRS (λ = 1.488 Å). Data sets were processed with *DENZO* and scaled with *SCALEPACK*.

3. Results and discussion

3.1. Ligand design and ligand selection

The largest family of cyclophilin inhibitors are related to the cyclic peptide cyclosporine A (Kallen *et al.*, 1998) and a number of weaker proline-containing oligopeptides also show inhibition (Kallen & Walkinshaw, 1992; Ke *et al.*, 1993). Recently, families of new non-peptide inhibitors have been synthesized (Wu *et al.*, 2003). In this work, we used the similarity search available in ISIS to identify molecules similar to the *cis*-proline found in a number of peptide ligands (Taylor *et al.*, 1997). One selection requirement was the presence of a hydrogen-bond donor to mimic the carbonyl O atom of the

Table 1
Crystallographic data for native hCypA and complexes.

	ETPIPG	ACMPIP	Native
Unit-cell parameters (Å)			
a	36.26	36.08	36.17
b	54.54	54.31	56.56
c	71.1	70.97	70.28
Space group	$P2_12_12_1$	$P2_12_12_1$	$P2_12_12_1$
Resolution (Å)	1.65	1.8	1.7
Temperature (K)	100	100	100
No. collected reflections	184971	103411	126301
Unique reflections	17641	13305	16375
Completeness of data (%)	90.2	98.7	99.5
Redundancy (%)	10.5	7.77	7.71
R_{merge}† (%)	4.0	5.0	5.1
Final R factor (all data) (%)	18.5	17.8	17.4
Free R factor (10% of data) (%)	22.5	23.1	21.9
Total non-H atoms	1535	1564	1458
Solvent sites	243	193	192
R.m.s.d. from ideality			
Bond lengths (Å)	0.007	0.007	0.007
Bond angles (°)	1.302	1.252	1.321
Mean temperature factors (Å²)			
Protein atoms	15.92	14.43	12.82
Ligand atoms (Å²)	20.95 (ALT1, 65%), 21.42 (ALT2, 35%)	25.09	
Water molecules (Å²)	35.26	31.17	30.72

† $R_{merge} = (\sum |I - \langle I \rangle| / \sum |I|)$, where I is the observed intensity and $\langle I \rangle$ is the average intensity from observations of symmetry-related reflections.

peptidylprolyl bond (Fig. 1). A hydrogen bond between this carbonyl O atom and the backbone N atom of Asn102 is conserved in all peptide–cyclophilin structures. The second feature was the requirement of a hydrophobic group to mimic the valine side chain of cyclosporin or the proline side chain of the peptide ligands. Two piperidine derivatives (Fig. 1) were selected according to these criteria.

The two published cyclophilin-binding assays make use of either fluorescence spectroscopy (Husi & Zurini, 1994) or enzymatic inhibition (Kofron *et al.*, 1991). The assay is based on the fact that chymotrypsin can only cleave the prolyl amide bond when in the *trans* coformation. Cyclophilins speed up the production of the *trans* conformer. The inhibitory activity of ACMPIP and ETPIPG has K_i values of 320 and 25 mM, respectively.

3.2. Crystal structures of native cyclophilin and two cyclophilin–ligand complexes

In order to make an accurate comparison of the structural effects of ligand binding, a high-resolution low-temperature
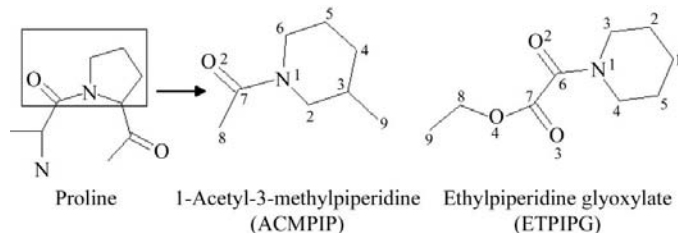

Figure 1
Formulae of the two ligands ACMPIP and ETPIPG, showing the similarity to *cis*-proline.

Table 2
Non-bonded contacts and hydrogen bonds in the active site for native hCypA, hCypA–ACMPIP and hCypA–ETPIPG.

hCypA atom	Native	Distance (Å)	ETPIPG	Distance (Å)	ACMPIP	Distance (Å)
Phe60 CZ			C1 (ALT2)	3.21	C4	3.49
Phe60 CE1			C1 (ALT2)	3.69	C9	3.54
Leu122 CD2	W121	3.71				
Arg55 NH2			C5 (ALT2)	3.77	C9	3.67
(ALT2) Arg55 NH2					C2	3.04
Arg55 NH2			C4 (ALT2)	3.91		
Arg55 NH1			C1 (ALT2)	3.05		
Arg55 NH2	W208	2.58	O4 (ALT1)	3.44		
Arg55 NE	W208	3.64				
Arg55 NH2			N1 (ALT2)	3.73		
Arg55 CD	W208	3.74				
Arg55 CDZ	W208	3.12				
Phe113 CE1	W106	3.71	C3 (ALT2)	3.48	C5	3.56
Phe113 CD1	W106	3.32	C3 (ALT2)	3.49	C5	3.64
Phe113 CD1			C8 (ALT1)	3.77	C6	3.61
			C2 (ALT2)	3.79		
Met61 CE	W106	3.08				
Gln63 OE1	W208	3.13	N1 (ALT2)	3.73		
Gln63 OE1			C7 (ALT1)	3.70		
Gln63 OE1	W106	2.92	O3 (ALT2)	3.73		
Gln63 OE1			O4 (ALT1)	3.70		
Gln63 OE1			C8 (ALT1)	3.45		
Gln63 CD	W106	3.55				
Gln63 NE2	W107	3.21	O2 (ALT1)	3.57		
			O3 (ALT2)	3.53		
Asn102 N	W105	2.90	C6 (ALT2)	3.77	O2	2.77
Asn102 N			O2 (ALT2)	2.71		
			O3 (ALT1)	3.07		
Asn102 O			O2 (ALT1)	3.78	O2	3.29
Asn102 O			C2 (ALT1)	3.26	C8	3.27
			C8 (ALT2)	3.67		
Asn102 O	W105	3.10	N1 (ALT1)	3.45		
			O4 (ALT2)	3.36		
Asn102 O	W107	3.68	C3 (ALT1)	3.62		
			C7 (ALT2)	3.21		
			C6 (ALT2)	3.77		
			C6 (ALT1)	3.56		
Asn102 O	W198	3.69	O3 (ALT1)	3.68		
			O2 (ALT2)	3.44		
His126 CE1	W105	3.35	C3 (ALT2)	3.74	C7	3.60
			O3 (ALT1)	3.13		
His126 CE1			O2 (ALT2)	3.26		
His126 CE1			C5 (ALT1)	3.71	O2	3.07
His126 CE1			C4 (ALT1)	3.67		
His126 CE1			C7 (ALT1)	3.76		
His126 CE1			C6 (ALT2)	3.46		
His126 CE1	W121	3.65	N1 (ALT2)	3.69		
His126 NE2	W121	2.86	C5 (ALT1)	3.75		
His126 NE2			C4 (ALT1)	3.75		
His126 ND1			O3 (ALT1)	3.68		
			O2 (ALT2)	3.73		
Ala101 C	W105	3.60	O3 (ALT1)	3.57	O2	3.41
Ala101 C			O2 (ALT2)	3.22		
Ala101 CA	W105	3.36	O3 (ALT1)	3.11	O2	3.14
Ala101 CA			O2 (ALT2)	2.84		
Ala101 CB	W105	3.38	O3 (ALT1)	3.18	O2	3.30
Ala101 CB	W106	3.55	O2 (ALT2)	2.92		
Solvent						
W93	W109	2.89				
W105	W106	2.84				
W105	W107	3.14				
W105	W198	2.97				
W106	W208	3.66				
W107	W208	3.74				
W109			O4 (ALT1)	3.20		
W121	W198	3.32				
W146	W198	3.60				

structure determination of native hCypA cyclophilin was carried out (Table 1). The low-temperature structure presented here enabled the location of native structure of four of the active-site water molecules W198, W106, W121 and
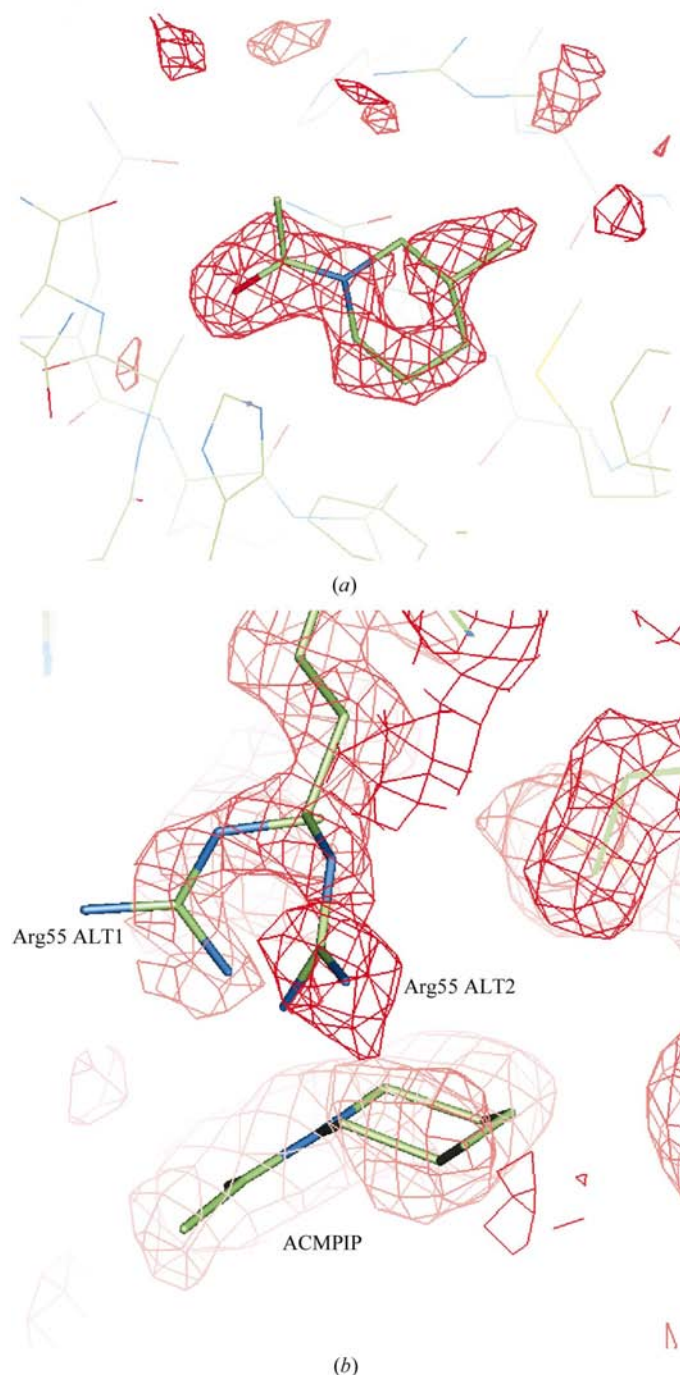

(a)

(b)

Figure 2
(a) $1F_o - 1F_c$ unbiased electron-density map for hCypA–ACMPIP contoured in red at 2.5σ. The map was calculated using data to 1.8 Å with phases from the partially refined 'native' hCypA structure which had not been contaminated with a ligand model. A stick representation of ACMPIP in its final refined orientation is shown for reference. (b) Final $2F_o - 1F_c$ electron-density map for hCypA–ACMPIP contoured in red at 1σ calculated using phases from all atoms including waters and ligand. The orientation is selected to show the alternative conformations of Arg55 in proximity to the ACMPIP ligand.
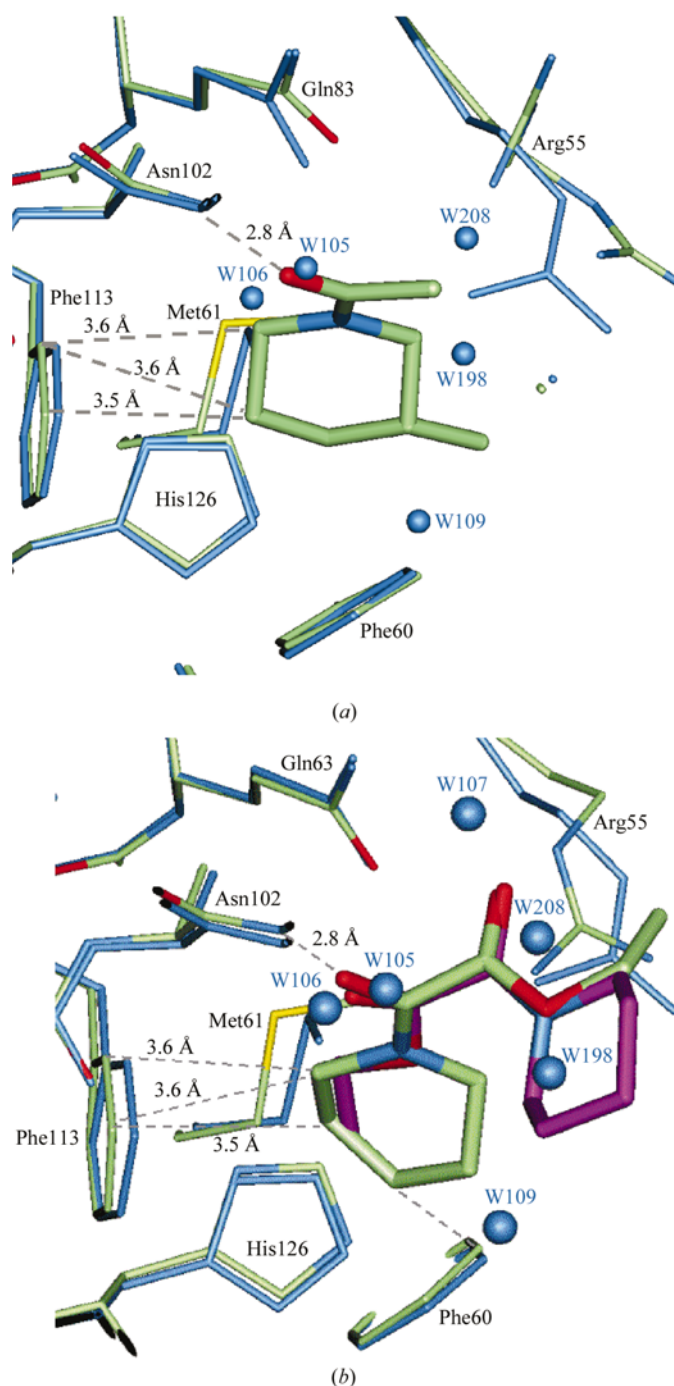

(a)

(b)

Figure 3
(a) Overlay of native hCypA (cyan) with hCypA–ACMPIP (atom-type colours). Close contacts between the ACMPIP ligand with surrounding atoms are shown. ACMPIP makes one hydrogen bond to Asn102 N (2.8 Å). The most hydrophobic part of the ACMPIP molecule (the methylpiperidine ring) fits into the hydrophobic pocket. van der Waals contacts are made from the ligand to the side chains of six amino acids (Arg55, Phe 60, Met61, Gln63, Phe113 and His126). (b) Overlay of native hCypA (cyan) with the hCypA–ETPIPG in both binding modes (ALT2, green; ALT1, purple). The main difference between the native protein structure and the structure with ETPIPG in the binding site is the movement of the side chain of Met61. The overall backbone conformations of the three structures are very similar. An r.m.s. fit of all protein atoms except residues 1–4, 67–76 and 162–165 between native and the ACMPIP complex is 0.286 Å and that between the ACMPIP and ETPIPG complexes is 0.367 Å.

W109 (Table 2) which were not observed in an earlier room-temperature structure (Ke *et al.*, 1991).
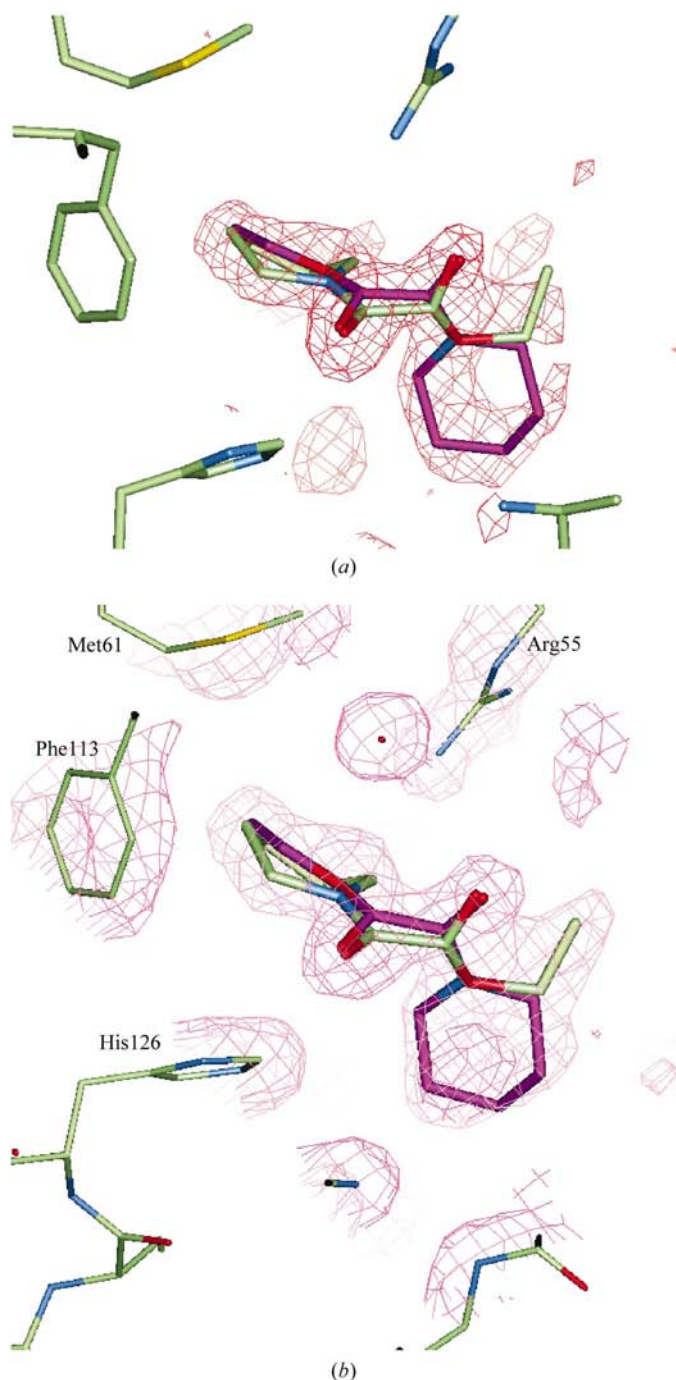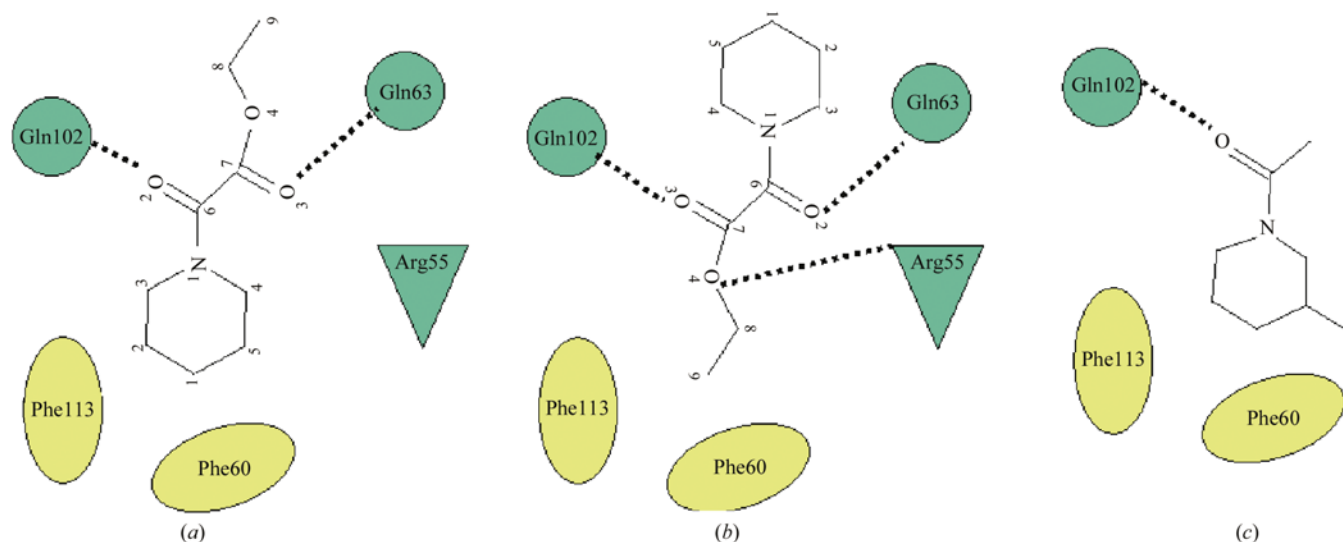

Figure 4
(*a*) $1F_o - 1F_c$ unbiased electron-density map for hCypA–ETPIPG contoured in red at 2.5σ. The map was calculated using data to 1.6 Å with phases from the partially refined 'native' hCypA structure which had not been contaminated with a ligand model. A stick representation of the two disordered ETPIPG molecules in their final refined orientations are overlaid: ALT1 (65% occupancy; C atoms purple) and ALT2 (35% occupancy; C atoms green). (*b*) Difference electron-density map ($2F_o - 1F_c$) for the refined ETPIPG–hCypA complex contoured at 1σ. Both water molecules and ligand were included in the phase calculation. The two orientations of ETPIPG are shown: ALT1 (65% occupancy; C atoms purple) and ALT2 (35% occupancy; C atoms green).

A hCypA–ACMPIP complex was prepared by soaking a crystal of native hCypA in a saturated solution of ACMPIP; an initial difference Fourier map showed clear electron density in the active site (Fig. 2) consistent with the ligand. The binding mode of ACMPIP mimics the binding of *cis*-proline ligands in a number of X-ray structures (Zhao & Ke, 1996; Kallen & Walkinshaw, 1992; Taylor *et al.*, 1997). A hydrogen bond between the amide carbonyl O atom of the ligand and the amide N atom of Asn102 (O$\cdots$N = 2.77 Å) provides the key recognition feature (Fig. 3*a*; Table 2). This hydrogen bond can only be formed by proline derivatives in the *cis* conformation. The well defined hydrophobic pocket in the active site is bounded by Phe60, Met61, Phe113 and Leu122 and is filled by the piperidine ring as predicted. Differences between the native protein structure and the structure with ACMPIP in the binding site are the movement of the side chain of Met61 observed in all other small ligand structures with hCypA, the replacement of five water molecules (W105, W106, W198, W109 and W208) by ACMPIP and the significantly different conformation of the Arg55 side chain (Fig. 3*a*).

The hCypA–ETPIPG complex was prepared by soaking a hCypA crystal in a saturated solution of ETPIPG. The complex with ETPIPG is found to adopt two different but overlapping orientations in the active site (Fig. 4). Different trial occupancies for the two ligand orientations were tested and individual atom *B* factors for each ligand were refined. Occupancies of 0.35 and 0.65 gave comparable *B* factors for the atoms in each ligand (Table 1). The lower (35%) occupancy orientation of the ligand (ALT2) is similar to the binding mode adopted by ACMPIP, with the piperidine ring fitting in the hydrophobic pocket lined by Phe113, Met61 and Phe60 (Figs. 3*b* and 5). The hydrogen bond between Asn102 N and the carbonyl O atom O2 (N$\cdots$O = 2.71 Å) is also conserved. The alternative orientation of the ligand (ALT1) has an occupancy of 65% and sits in a rotated orientation in the binding pocket such that that the ethyl group now occupies the hydrophobic pocket and the piperidine group is essentially exposed to solvent. The approximate twofold symmetry of the ETPIPG ligand, however, means that the binding sites in the active-site pocket are filled by pseudo-symmetry-related atoms (Figs. 3*b* and 5). The ALT1 mode allows all three O atoms in the glyoxylate group to form potential hydrogen bonds with Asn102, Arg55 and Gln63. There is also a close and favourable contact between the backbone carbonyl O atom of Asn102 and the amide N atom of the piperidine ring (Fig. 5; Table 2). These additional electrostatic interactions are presumably at the expense of moving the hydrophobic piperidine ring out of the hydrophobic pocket. The conformations of the ethylglyoxylate molecule is similar in both of its binding modes and both maintain an expected O=C−C=O torsion angle of 90° for the α–β carbonyl O atoms. The only significant difference between the binding pockets of the two structures is in the conformation of the side chain of Arg55, which is pushed away from the binding site in the ACMPIP structure but is involved in ligand binding in the ETPIPG structure.

Figure 5
Diagrammatic representation of the major ligand–protein interactions. Hydrogen bonds are shown as dotted lines. The hydrophobic pocket is primarily bounded by the side chains of Phe113 and Phe60, which are shown as green ovals.

3.3. Factors affecting the strength of protein–ligand interactions

A number of attempts have been made to estimate ligand-binding strength as a linear sum of factors, including van der Waals contacts, hydrogen bonds, rotational and translational entropy changes (Klebe & Bohm, 1997). For families of related ligands binding to the same enzyme, it is possible to obtain good correlations between calculated and measured binding constants (Verkhivker et al., 1995; Muegge et al., 1999; Goodsell et al., 1996; Knegtel et al., 1999; Davies et al., 1999). The combined structural and enzymatic data available is relatively sparse, with examples from about 20 different enzyme–ligand complexes (Bohm, 1994). The complex of cancanavalin A with methylmannoside (Naismith et al., 1994), which has an experimental dissociation constant of 0.95 mM (corresponding to a binding energy of -62.7 kJ mol^{-1}), is one of the weakest binding complexes to have been jointly characterized unambiguously by X-ray crystallography and binding studies. The cyclophilin structures presented here are orders of magnitude weaker than this: the K_i values of ACMPIP and ETPIPG are 320 and 25 mM, respectively, corresponding to binding energies of -2.4 and -9 kJ mol^{-1}.

The buried surface of the ligand provides some measure of the van der Waals interaction energy. The buried surface areas of ACMPIP and ETPIPG are 205 and 189 (ALT1) and 196 Å^2 (ALT2), respectively. Estimates of the surface-energy contributions to binding energy vary between about -0.2 and -0.5 kJ mol^{-1} Å^{-2} (Bohm, 1998; Burkhard et al., 2000). This gives binding-energy estimates of between 40 and 100 kJ mol^{-1} for both ligands, although the ACMPIP ligand has a marginally higher solvent-excluded binding surface but binds significantly more weakly. For both ligands the calculated enthalpic terms are significantly greater than the observed binding strengths, which suggests that a number of unfavourable energy effects must also play a role.

One major energy cost for ligand binding is caused by the break-up and displacement of the water structure in the active site. ACMPIP displaces five water molecules and ETPIPG displaces six water molecules from the active site (Figs. 3a and 4b). In the native structure, W105 is hydrogen bonded to Asn102 and in both cyclosporin A complexes and the piperidine family of cyclophilin ligands, W105 is mimicked by a carbonyl O atom. One difference between the binding of the two ligands is the number of (weak) but direct hydrogen bonds between the ligand and the protein (Table 2). In ACMPIP and ETPIPG there is one direct hydrogen bond to Asn102 N and in both binding modes of the ETPIPG there are an additional one or two weak hydrogen bonds. Hydrogen bonds are estimated to contribute about -5 kJ mol^{-1} (Klebe & Bohm, 1997) to the binding energy. On binding piperidyl ligands to cyclophilin, one good hydrogen bond is made, but networks of more than 11 water–protein and water–water hydrogen bonds have been lost in the two complexes. There are also additional ripple effects at the edge of the active site where more distant hydrogen-bonding water partners are perturbed by side-chain movements.

Induced conformational change in protein side chains may also reduce the energy of binding. Three amino-acid side chains in proximity to the active site (Met61, Arg55 and Gln63) show significantly different conformations in the three structures (Figs. 3a and 3b). The Met61 side chain adopts a different conformation in both structures, with a change in χ^3 of about 120°. The catalytically important residue Arg55 forms hydrogen bonds to most peptide ligands (Taylor et al., 1997). There is no hydrogen-bonding possibility with ACMPIP and the guanidinium group is twofold disordered in this complex. ETPIPG does not have the additional bulk of the C3 methyl group on the piperidine ring, which leaves enough room for the Arg55 side chain to adopt a single conformation similar to that found in the native hCypA structure. It seems likely that

the repulsion between the methyl group of ACMPIP and Arg55 accounts for a major difference between the K_i values of the two piperidyl ligands. The entropic contribution to binding energy from the twofold-disordered ETPIPG structure is difficult to assess. It has been observed previously that ligands can frequently bind in different modes (Mattos *et al.*, 1994).

3.4. The role of weakly binding pro-ligands in the development of pharmaceutical leads

The success of 'SAR by NMR' in designing tight-binding FK506 binding protein ligands (Shuker *et al.*, 1996) highlights the importance of making use of weakly binding pro-ligands. The major problem in studying the interaction of such weakly binding ligands is being able to reach a sufficiently high ligand concentration. NMR studies of lysozyme have been carried out in high concentrations (1–13 M) of organic solvents including DMSO, methanol and acetonitrile (Liepinsh & Otting, 1997). X-ray studies of elastase crystals soaked in acetonitrile have also been used to map possible binding sites (Allen *et al.*, 1996).

The micromolar criterion used in high-throughput screening searches for new ligands requires ligands to have a dissociation energy of less than -33.6 kJ mol^{-1}. It is unlikely that small ligands will bind with this energy, principally because of the competition with water. Both the entropy and enthalpy of a small ligand are comparable to those of bound water. Thus, the combined effects of a small binding-surface area and the competition with water normally require organic ligands to be of a molecular weight greater than 300 Da for micromolar binding. Small-molecule drugs typically have molecular weights of between 300 and 700 Da.

The structures presented here show that it is possible to obtain ordered X-ray structures for weakly binding low-molecular-weight ligands using conventional crystal-soaking methods. Once a pharmacophore can be accurately located in the binding pocket of an enzyme, the structure can be used as template for the design of larger (tighter binding) chemical derivatives.

References

Allen, K. N., Bellamacina, C. R., Ding, X. C., Jeffery, C. J., Mattos, C., Petsko, G. A. & Ringe, D. (1996). *J. Phys. Chem.* **100**, 2605–2611.

Berman, H. M., Westbrook, J., Feng, Z., Gilliland, G., Bhat, T. N., Weissig, H., Shindyalov, I. N. & Bourne, P. E. (2000). *Nucleic Acids Res.* **28**, 235–242.

Beveridge, T. & Calne, R. Y. (1995). *Transplantation*, **59**, 1568–1570.

Bleicher, K. H., Bohm, H. J., Muller, K. & Alanine, A. I. (2003). *Nature Rev. Drug Discov.* **2**, 369–378.

Blundell, T. L., Jhoti, H. & Abell, C. (2003). *Nature Rev. Drug Discov.* **1**, 45–54.

Bohm, H. J. (1994). *J. Comput.-Aided Mol. Des.* **8**, 243–256.

Bohm, H. J. (1998). *J. Comput.-Aided Mol. Des.* **12**, 309–323.

Bohm, H. J. & Klebe, G. (1996). *Angew. Chem. Int. Ed. Engl.* **35**, 2589–2614.

Burkhard, P., Taylor, P. & Walkinshaw, M. D. (2000). *J. Mol. Biol.* **295**, 953–962.

Davies, T. G., Hubbard, R. E. & Tame, J. R. H. (1999). *Protein Sci.* **8**, 1432–1444.

Davis, A. M. & Teague, S. J. (1999). *Angew. Chem. Int. Ed. Engl.* **38**, 737–749.

Galat, A. & Metcalfe, S. M. (1995). *Prog. Biophys. Mol. Biol.* **63**, 67–118.

Glen, R. C. & Allen, S. C. (2003). *Curr. Med. Chem.* **10**, 763–777.

Goodsell, D. S., Morris, G. M. & Olson, A. J. (1996). *J. Mol. Recogn.* **9**, 1–5.

Husi, H. & Zurini, M. G. M. (1994). *Anal. Biochem.* **222**, 251–255.

Kallen, J., Mikol, V., Taylor, P. & Walkinshaw, M. D. (1998). *J. Mol. Biol.* **283**, 435–449.

Kallen, J. & Walkinshaw, M. D. (1992). *FEBS Lett.* **300**, 286–290.

Ke, H. M., Mayrose, D. & Cao, W. (1993). *Proc. Natl Acad. Sci. USA*, **90**, 3324–3328.

Ke, H. M., Zydowsky, L. D., Liu, J. & Walsh, C. T. (1991). *Proc. Natl Acad. Sci. USA*, **88**, 9483–9487.

Klebe, G. & Bohm, H. J. (1997). *J. Recept. Signal Transduction Res.* **17**, 459–473.

Knegtel, R. M. A., Bayada, D. M., Engh, R. A., von der Saal, W., van Geerestein, V. J. & Grootenhuis, P. D. J. (1999). *J. Comput.-Aided Mol. Des.* **13**, 167–183.

Kofron, J. L., Kuzmic, P., Kishore, V., Colonbonilla, E. & Rich, D. H. (1991). *Biochemistry*, **30**, 6127–6134.

Liepinsh, E. & Otting, G. (1997). *Nature Biotechnol.* **15**, 264–268.

Lilie, H., Lang, K., Rudolph, R. & Buchner, J. (1993). *Protein Sci.* **2**, 1490–1496.

Mattos, C., Rasmussen, B., Ding, X. C., Petsko, G. A. & Ringe, D. (1994). *Nature Struct. Biol.* **1**, 55–58.

Meyer, B. & Peters, T. (2003). *Angew. Chem. Int. Ed. Engl.* **42**, 864–890.

Muegge, I., Martin, Y. C., Hajduk, P. J. & Fesik, S. W. (1999). *J. Med. Chem.* **42**, 2498–2503.

Naismith, J. H., Emmerich, C., Habash, J., Harrop, S. J., Helliwell, J. R., Hunter, W. N., Raftery, J., Kalb, A. J. & Yariv, J. (1994). *Acta Cryst.* D**50**, 847–858.

Page, A. P., Kumar, S. & Carlow, C. K. S. (1995). *Parasitol. Today*, **11**, 385–388.

Ringe, D. & Mattos, C. (1999). *Med. Res. Rev.* **19**, 321–331.

Shuker, S. B., Hajduk, P. J., Meadows, R. P. & Fesik, S. W. (1996). *Science*, **274**, 1531–1534.

Taylor, P., Husi, H., Kontopidis, G. & Walkinshaw, M. D. (1997). *Prog. Biophys. Mol. Biol.* **67**, 155–181.

Verkhivker, G., Appelt, K., Freer, S. T. & Villafranca, J. E. (1995). *Protein Eng.* **8**, 677–691.

Wu, Y. Q., Belyakov, S., Choi, C., Limburg, D., Thomas, B. E., Vaal, M., Wei, L., Wilkinson, D. E., Holmes, A., Fuller, M., McCormick, J., Connolly, M., Moeller, T., Steiner, J. & Hamilton, G. S. (2003). *J. Med. Chem.* **46**, 1112–1115.

Zhao, Y. D. & Ke, H. M. (1996). *Biochemistry*, **35**, 7362–7368.